Available online at www.sciencedirect.com
ScienceDirect
Mechanism and Machine Theory 42 (2007) 66–81
Mechanism and Machine Theory
www.elsevier.com/locate/mechmt

A new and efficient algorithm for the inverse kinematics of a general serial 6*R* manipulator

Manfred L. Husty *, Martin Pfurner, Hans-Peter Schröcker

University Innsbruck, Institute of Engineering Mathematics, Geometry and Computer Science, Technikerstraße 13, A6020 Innsbruck, Austria

Received 19 January 2006; received in revised form 7 February 2006; accepted 13 February 2006
Available online 17 April 2006

Abstract

In this paper a new and very efficient algorithm to compute the inverse kinematics of a general 6*R* serial kinematic chain is presented. The main idea is to make use of classical multidimensional geometry to structure the problem and to use the geometric information before starting the elimination process. For the geometric pre-processing we utilize the Study model of Euclidean displacements, sometimes called kinematic image, which identifies a displacement with a point on a six dimensional quadric S_6^2 in seven dimensional projective space P^7. The 6*R*-chain is broken up in the middle to form two open 3*R*-chains. The kinematic image of a 3*R*-chain turns out to be a Segre-manifold consisting of a one parameter set of 3-spaces. The intersection of two Segre-manifolds and S_6^2 yields 16 points which are the kinematic images representing the 16 solutions of the inverse kinematics. Algebraically this procedure means that we have to solve a system of seven linear equations and one resultant to arrive at the univariate 16 degree polynomial. From this step in the algorithm we get two out of the six joint angles and the remaining four angles are obtained straight forward by solving the inverse kinematics of two 2*R*-chains.
© 2006 Elsevier Ltd. All rights reserved.

2000 MSC: 70B15; 53A17

Keywords: 6*R* manipulator; Inverse kinematics; Multidimensional geometry; Study representation; Kinematic mapping; Segre manifold

1. Introduction

The inverse kinematics of general 6*R* linkages attracted many excellent researchers of the kinematics community in the end 1980s and beginning 1990s of the last century. At that time this problem was considered to be the most difficult among all open problems in kinematics. In 1988 Lee and Liang [1] came up with a solution which was not very transparent, so that most the time Raghavan and Roth's [2] solution from 1990 is cited in the textbooks. There were many attempts to improve the algorithm. For example, Ghazvini [3]

* Corresponding author. Tel.: +43 512 507 6830; fax: +43 512 507 2709.
E-mail address: manfred.husty@uibk.ac.at (M.L. Husty).

0094-114X/$ - see front matter © 2006 Elsevier Ltd. All rights reserved.
doi:10.1016/j.mechmachtheory.2006.02.001

reduced the problem to the solution of a generalized eigenproblem. An explicit enumeration and recognition of all developments would be to extensive. An overview on the development over the years can be found in [4].

To the authors surprise the geometric structure of the problem was never really revealed. We always had the feeling that the manipulations with the non-linear algebraic equations, describing the problem were somehow as luck would have it, although with great intuition. To our opinion the method of kinematic mapping combined with classical results of multidimensional geometry bear the tools to give the necessary insight to the problem.

The paper is organized as follows: in Section 2 we introduce the mathematical and geometrical tools. We recall the notation to describe serial chains and discuss the Study model of Euclidean displacements. In Section 3 we introduce the constraint manifold of a spatial $3R$-chain, which turns out to be the key to the solution of the inverse kinematics. This constraint manifold is a well known construct in multidimensional geometry: a so called Segre-manifold. Some of its properties are described in Section 4. In Section 5 we apply the results of Sections 3 and 4 and give a new algorithm to solve the inverse kinematics of a general $6R$-chain. In Appendix A a numerical example for this algorithm is given.

2. Mathematical framework

2.1. Design parameters

A serial $6R$ manipulator is composed of a sequence of seven links connected by six revolute joints. The links are numbered such that link zero constitutes the base of the robot and link six is the terminal link where the end effector is located. Joint i connects link i and link $i-1$ and the variable joint parameter (rotation angle) is denoted by u_i. In order to define the relationship between the location of links, we assign a coordinate frame Σ_i attached to link i, such that the z_i-axes coincide with the axes of joint i, the x_i-axes are aligned with the common normal of link i and $i+1$. The y_i-axes lie such that these three axes form a right-hand coordinate frame. Then the relative displacement of Σ_6 with respect to the fixed frame Σ_0 can be computed by linking all relative displacements of Σ_i with respect to Σ_{i-1} and is therefore given by the matrix:[1]

$$\mathbf{D} = \mathbf{M}_1 \cdot \mathbf{G}_1 \cdot \mathbf{M}_2 \cdot \mathbf{G}_2 \cdot \mathbf{M}_3 \cdot \mathbf{G}_3 \cdot \mathbf{M}_4 \cdot \mathbf{G}_4 \cdot \mathbf{M}_5 \cdot \mathbf{G}_5 \cdot \mathbf{M}_6 \cdot \mathbf{G}_6, \tag{1}$$

$$\mathbf{M}_i = \begin{bmatrix} 1 & 0 & 0 & 0 \\ 0 & \cos(u_i) & -\sin(u_i) & 0 \\ 0 & \sin(u_i) & \cos(u_i) & 0 \\ 0 & 0 & 0 & 1 \end{bmatrix}, \quad \mathbf{G}_i = \begin{bmatrix} 1 & 0 & 0 & 0 \\ a_i & 1 & 0 & 0 \\ 0 & 0 & \cos(\alpha_i) & -\sin(\alpha_i) \\ d_i & 0 & \sin(\alpha_i) & \cos(\alpha_i) \end{bmatrix}$$

for $i = 1, \ldots, 6$, where α_i is the twist angle between the z-axes of the links $i-1$ and i, a_i is the offset distance between the same axes and d_i is the translational distance of two common normals of the z-axes of link i with the adjacent z-axes of links $i-1$ and $i+1$. As usual the design parameters are called Denavit–Hartenberg parameters (DH-parameters). Establishing the transformation matrices we have made use of the fact that every serial chain can be brought to a position where all revolute axes are parallel to one plane. This configuration is used as home position of the chain. It is easy to see that this home position can be achieved by the following algorithm: Choose the plane normal to the common perpendicular of the first two revolute axes and fix the first one. Now the remaining manipulator axes are rotated about the second joint until the third axis is parallel to the chosen plane. Now the first three axes are fixed and the next axis is rotated to a position parallel to the chosen plane. This process is repeated until all axes are parallel to the plane. The result of this process is shown in Fig. 1 in four different views. In this figure the yz-plane of Σ_0 is chosen to be parallel to all axes. Note that in the home position all Denavit–Hartenberg parameters can be seen in true shape: The common normals of the rotation axes a_i are parallel to the top view and the front view plane and the angles α_i between the rotation axes and the offsets d_i are in true shape in the side view. (Because the picture is described by side not right view.)

[1] Throughout the whole paper the European notation is used and the first coordinate is the homogenizing coordinate.

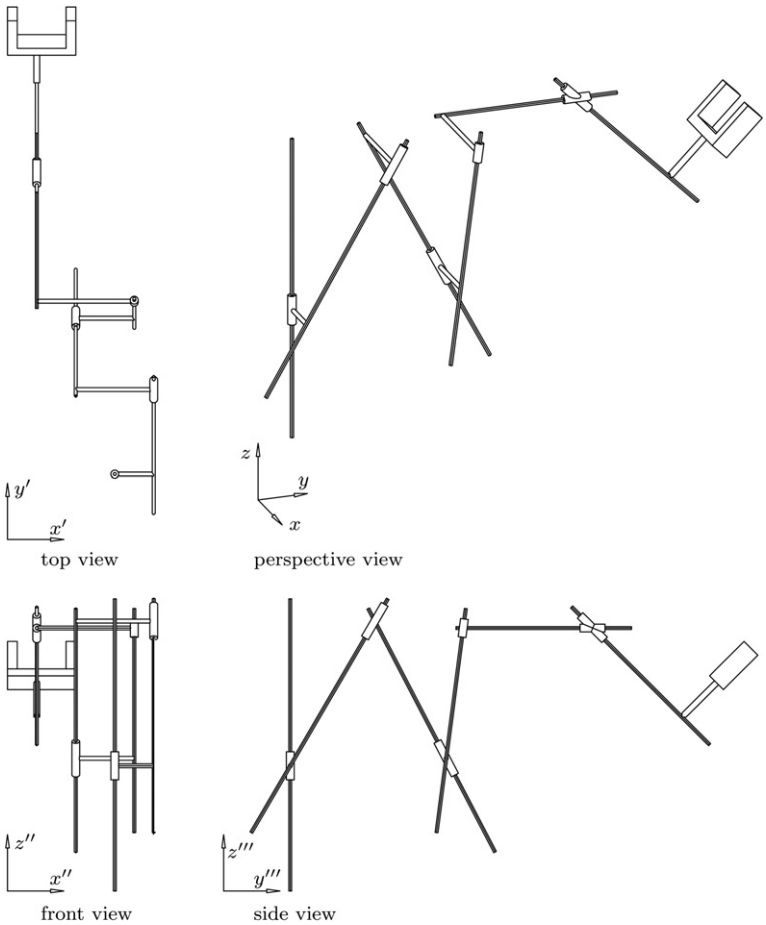

Fig. 1. General 6*R* manipulator in home position, all axes parallel to *yz*-plane.

Furthermore this home pose shows that no serial manipulator is singularity free, because in this home position all axes intersect the line at infinity of the chosen plane and belong therefore to a special linear complex. The determinant of the Jacobian matrix of the manipulator vanishes in this position. It should be noted that this home position – although being singular – does not at all restrict the generality of the following computations. It only reduces the complexity of the equations.

2.2. Study-model of SE(6)

Euclidean displacements $\mathscr{D} \in \mathrm{SE}(6)$ can be described by (see [5,6])

$$\mathscr{D} : \mathbf{x}' = \mathbf{A}\mathbf{x} + \mathbf{t}, \tag{2}$$

where $\mathbf{x}'$ resp. $\mathbf{x}$ represent a point in the fixed resp. moving frame, $\mathbf{A}$ is a 3×3 proper orthogonal matrix and $\mathbf{t} = [t_1, t_2, t_3]^{\mathrm{T}}$ is the translation vector, connecting the origins of moving and fixed frame. Expanding the dual quaternion representation [5, Section 3.3.2] and using an operator approach the matrix operator corresponding to the normalized dual quaternion $\mathbf{q} = [x_0, x_1, x_2, x_3] + \varepsilon[y_0, y_1, y_2, y_3]$ is given by

$$\mathbf{M} := \begin{bmatrix} 1 & 0 & 0 & 0 \\ t_1 & x_0^2 + x_1^2 - x_3^2 - x_2^2 & -2x_0x_3 + 2x_2x_1 & 2x_3x_1 + 2x_0x_2 \\ t_2 & 2x_2x_1 + 2x_0x_3 & x_0^2 + x_2^2 - x_1^2 - x_3^2 & -2x_0x_1 + 2x_3x_2 \\ t_3 & -2x_0x_2 + 2x_3x_1 & 2x_3x_2 + 2x_0x_1 & x_0^2 + x_3^2 - x_2^2 - x_1^2 \end{bmatrix}, \tag{3}$$

where

$$\begin{aligned} t_1 &= 2x_0y_1 - 2y_0x_1 - 2y_2x_3 + 2y_3x_2, \\ t_2 &= 2x_0y_2 - 2y_0x_2 - 2y_3x_1 + 2y_1x_3, \\ t_3 &= 2x_0y_3 - 2y_0x_3 - 2y_1x_2 + 2y_2x_1. \end{aligned} \tag{4}$$

The point $[x, y, z]^{\mathrm{T}}$ is transformed to $[x', y', z']^{\mathrm{T}}$ according to

$$[1, x, y, z]^{\mathrm{T}} = \mathbf{M} \cdot [1, x', y', z']^{\mathrm{T}}.$$

The entries $[x_i, y_i]$ in the transformation matrix $\mathbf{M}$ have to fulfill the quadratic identity

$$x_0y_0 + x_1y_1 + x_2y_2 + x_3y_3 = 0 \tag{5}$$

and at least one x_i is different from 0. The lower right 3×3 sub-matrix of $\mathbf{M}$ is an element of the special orthogonal group $\mathrm{SO}(3)^+$ and the x_i are the Euler parameters. This representation of Euclidean displacements is sometimes called Study representation and the parameters x_i, y_i are called Study parameters. This allows the following multidimensional geometric interpretation: Eq. (5) defines a six dimensional quadric hyper-surface in a seven dimensional projective space P^7. This quadric S_6^2 is called Study quadric and serves as a point model for Euclidean displacements. The quadric S_6^2 is of hyperbolic type and has the following properties:

(1) The maximal linear spaces on S_6^2 are three dimensional (generator spaces).
(2) Each tangent space cuts S_6^2 in a five dimensional cone.
(3) The generator space $x_0 = x_1 = x_2 = x_3 = 0$ is one of the 3-spaces mentioned above but it does not represent regular displacements, because in this space all Euler parameters are zero. Therefore this space has to be cut out of S_6^2. A quadric with one generator space removed is called sliced.

A detailed treatment of more properties of S_6^2 can be found in [7, Chapter 10].

The mapping

$$\begin{aligned} &\kappa : \mathscr{D} \to P \in P^7 \\ &\mathbf{M}(x_i, y_i) \to [x_0 : x_1 : x_2 : x_3 : y_0 : y_1 : y_2 : y_3]^{\mathrm{T}} \neq [0 : 0 : 0 : 0 : 0 : 0 : 0 : 0]^{\mathrm{T}} \end{aligned} \tag{6}$$

is called *kinematic mapping* and maps each Euclidean displacement $\mathscr{D}$ to a point P on $S_6^2 \subset P^7$.

Given a displacement $\mathscr{D}$ as in Eq. (2) it is straightforward to compute the Study parameters x_i, y_i. One can use one of the formulas (7) to compute the Euler parameters x_i directly from the 3×3 lower right sub-matrix $\mathbf{A} = (a_{ij})_{i,\ j=1,\ldots,3}$ of $\mathbf{M}$:

$$\begin{aligned} x_0 : x_1 : x_2 : x_3 &= 1 + a_{11} + a_{22} + a_{33} : a_{32} - a_{23} : a_{13} - a_{31} : a_{21} - a_{12} \\ &= a_{32} - a_{23} : 1 + a_{11} - a_{22} - a_{33} : a_{12} + a_{21} : a_{31} + a_{13} \\ &= a_{13} - a_{31} : a_{12} + a_{21} : 1 - a_{11} + a_{22} - a_{33} : a_{23} + a_{32} \\ &= a_{21} - a_{12} : a_{31} + a_{13} : a_{23} + a_{32} : 1 - a_{11} - a_{22} + a_{33}. \end{aligned} \tag{7}$$

These formulas are already due to Study [8]. If $\mathbf{A}$ is non-symmetric, we can always take the first formula of (7). If $\mathbf{A}$ is symmetric, then it describes a rotation through an angle of π and the first formula fails. In this case we can always resort to one of the three remaining formulas. The y_i are given by

$$\begin{aligned} y_0 &= -\frac{1}{2}(t_3x_3 + t_2x_2 + t_1x_1), \quad y_1 = -\frac{1}{2}(t_3x_2 - t_2x_3 - t_1x_0), \\ y_2 &= -\frac{1}{2}(-t_3x_1 + t_1x_3 - t_2x_0), \quad y_3 = -\frac{1}{2}(-t_3x_0 + t_2x_1 - t_1x_2). \end{aligned} \tag{8}$$

3. Kinematic image of a 3*R* serial chain

The most important step in the proposed algorithm for the inverse kinematics of an open 6*R*-chain, developed in Section 5, is the decomposition of the 6*R*-chain into two 3*R*-chains. Therefore, at first we will study the kinematic image of the 3*R*-chain and derive some of its geometric properties.

Given the design (the DH-parameters) of an arbitrary $3R$-chain we can compute the relative position of the end-effector frame Σ with respect to a base frame Σ_0 in dependence of three rotation angles u_1, u_2, u_3. Therefore, the constraint manifold of a $3R$-chain, representing all poses the frame Σ can attain is a 3-manifold in the kinematic image space.

It is known (see [7]) that the constraint manifold representing a $2R$-chain in the kinematic image space is the intersection of a 3-space T with the Study quadric S_6^2. This fact has been used in [9] to derive a new method for the synthesis of Bennett mechanisms. The intersection of S_6^2 and T is again a quadric surface.

If we fix one of the three revolute joints of the $3R$-chain by fixing one parameter, say u_3, we get a $2R$-chain. Its kinematic image lies in a 3-space T. Hence, the constraint manifold of the $3R$-chain is the intersection of the Study-quadric S_6^2 with a one parameter set of 3-spaces $T(u_3)$.

If we fix two of the three revolute joints of the $3R$-chain by fixing the parameters u_1 and u_2, we get a pure rotation about the third revolute axis. This rotation maps to a line l on the Study quadric. The line l itself depends on the two parameters u_1 and u_2; therefore we write $l = l(u_1, u_2)$. The points on l are parameterized by u_3. We have a closer look at this parametrization.

The parametric representation of the constraint manifold of the $3R$-chain in kinematic image space, as computed via (7) and (8), reads $\mathbf{p}(u_1, u_2, u_3)$. We apply the half-tangent substitution $v_i = \tan(u_i/2)$, thus obtaining a rational parametric representation $\mathbf{p}(v_1, v_2, v_3)$ of degree four. Fixing v_1 and v_2 yields a rational parametrization $\mathbf{p}(v_3)$ of the straight line $l(v_1, v_2)$.

Lemma 1. *For any v_1, v_2, the parametric representation $\mathbf{p}(v_3)$ of $l(v_1, v_2)$ is linear in v_3.*

Proof. After half-tangent substitution, kinematic mapping and multiplication with the least common multiple of the denominator polynomials, the homogeneous parametric representation $\mathbf{p}(v_3)$ is polynomial and of degree four – at least formally. Using a computer algebra system one finds that all eight coordinate polynomials of $\mathbf{p}(v_3)$ have a common divisor $d(v_3)$ of degree three. Hence, we can divide $\mathbf{p}(v_3)$ by $d(v_3)$ without destroying its polynomial character. The resulting parametric representation is linear in v_3. □

The 3-spaces $T(v_3)$ can be generated in the following way: We choose four fixed straight lines $l(v_{1,i}, v_{2,i})$, parameterized by $\mathbf{p}_i(v_3)$ $(i = 1, \ldots, 4)$. Every 3-space $T(v_3)$ is spanned by $\mathbf{p}_1(v_3), \ldots, \mathbf{p}_4(v_3)$. On the other hand, a straight line $l(v_1, v_2)$ is the span of two points $\mathbf{p}_j(v_1, v_2) \in T(v_{3,j})$. The relation between the points $\mathbf{p}_j(v_1, v_2)$ can be extended to a unique projective transformation $\pi : T(v_{3,1}) \to T(v_{3,2})$ such that $\pi(\mathbf{p}_1(v_1, v_2)) = \mathbf{p}_2(v_1, v_2)$ for all v_1, v_2. Any straight line spanned by corresponding points $\mathbf{x} \in T(v_{3,1})$ and $\pi(\mathbf{x}) \in T(v_{3,2})$ intersects all 3-spaces $T(v_3)$ and any four of these lines can be used to generate the 3-spaces $T(v_3)$.

The one parameter set of 3-spaces $T(v_3)$ generated as above is known in geometry as a *Segre manifold*. A Segre manifold is also defined as topological product of two linear spaces, i.e., the manifold of all ordered pairs of points of both spaces [10, p. 569].

So far, we always fixed the rotation angle $v_3 = \tan(u_3/2)$ of the third revolute joint, thus obtaining a Segre manifold that will be denoted by SM_3. Of course we can also fix v_1 or v_2. This yields two different one parameter sets of 3-spaces and two different Segre manifolds SM_3', SM_3''. This fact will be important for the inverse kinematics algorithm in Section 5 (see Remark 9).

We summarize the above considerations in

Theorem 2. *The constraint manifold of a $3R$-chain is the intersection of the Study quadric with a Segre manifold SM_3 (SM_3', SM_3''), generated by two projectively coupled 3-spaces $T_1, T_2 \subset P^7$. The intersection of T_i with the Study quadric S_6^2 is the kinematic image of a $2R$-chain obtained by fixing the rotation angles u_3 (u_1, u_2) of the $3R$-chain.*

A symbolic sketch of SM_3 is depicted in Fig. 2.

Corrollary 3. *The constraint manifold of a $3R$-chain is the intersection of any two of the Segre manifolds SM_3, SM_3', SM_3''.*

Proof. We consider the Segre manifolds SM_3' and SM_3''. They are swept by 3-spaces $T'(v_1)$ and $T''(v_2)$. The intersection of $T'(v_1)$ and $T''(v_2)$ is the straight line $l(v_1, v_2)$. The union of all straight lines $l(v_1, v_2)$ is precisely the intersection of SM_3 with the Study quadric S_6^2, i.e., the constraint manifold of the $3R$-chain. □

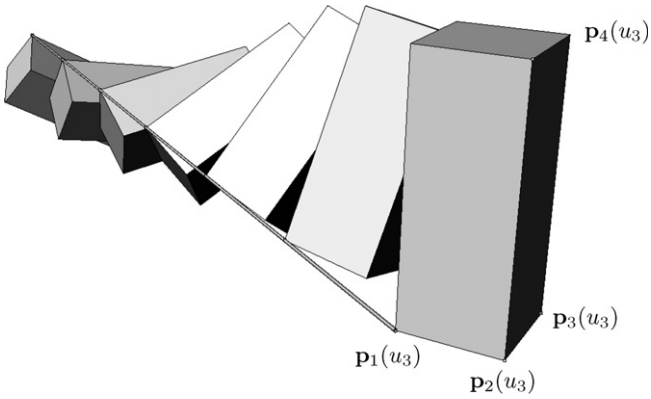

Fig. 2. Symbolic figure of SM_3.

4. Different representations of the Segre manifold

In this section we describe different representations of the Segre manifold SM_3. Having more than one representation at hand is advantageous, since the representation can be chosen according to the specific problem. We will present examples of this fact.

4.1. Parametric representation, span of points

We can view SM_3 as generated by two projectively coupled 3-spaces or four projectively coupled straight lines. This can be used to find a parametric representation of SM_3.

Denote the four straight lines by l_i and let $\mathbf{p}_i(v_3) = T(v_3) \cap l_i$. Because of Lemma 1 we may assume that $\mathbf{p}_i(v_3)$ is linear in v_3. Now the points of SM_3 are described by

$$SM_3\colon\ \mathbf{x} = \sum_{i=1}^{4} \lambda_i \mathbf{p}_i(v_3),$$

where $[\lambda_1, \lambda_2, \lambda_3, \lambda_4]^{\mathrm{T}}$ is a homogeneous quartuple.

In this representation, the algebraic degree of SM_3 is easily computed. It is defined as the number of intersection points of SM_3 and a generic 3-space $U \subset P^7$ [11]. Let U be the span of $\mathbf{u}_1, \ldots, \mathbf{u}_4$. U and $T(v_3)$ intersect if and only if

$$\det(\mathbf{p}_1(v_3), \mathbf{p}_2(v_3), \mathbf{p}_3(v_3), \mathbf{p}_4(v_3), \mathbf{u}_1, \mathbf{u}_2, \mathbf{u}_3, \mathbf{u}_4) = 0. \tag{9}$$

(9) is a polynomial of degree four in v_3. Hence there exist four intersection points of SM_3 and T: *The algebraic degree of* SM_3 *is four.*

4.2. Algebraic equations

In order to find a set of algebraic equations of SM_3 we fix two parameter values $v_{3,1}$ and $v_{3,2}$ and let $\mathbf{p}_{i,j} = \mathbf{p}_i(v_j)$ for $i = 1, \ldots, 4$ and $j = 1, 2$. In a projective coordinate frame with base points $\mathbf{p}_{1,1}, \ldots, \mathbf{p}_{4,1}$, $\mathbf{p}_{1,2}, \ldots, \mathbf{p}_{4,2}$, we use homogeneous coordinate vectors $[\xi_0 : \ldots : \xi_3 : \eta_0 : \ldots : \eta_3]^{\mathrm{T}}$. In this frame, the algebraic equations of SM_3 read

$$\det \begin{bmatrix} \xi_i & \eta_i \\ \xi_j & \eta_j \end{bmatrix} = 0, \quad i, j \in \{0, \ldots, 3\} \tag{10}$$

(see [10, p. 569]). Note that only three of these quadratic equations are independent. Therefore, SM_3 is the intersection of three hyper-quadrics. In order to find the equations of SM_3 in the original coordinate frame of P^7, we have to apply the transformation $\mathbf{y} = \mathbf{P}\mathbf{x}$ where $\mathbf{P}$ is the matrix

$$\mathbf{P} = [\mathbf{p}_{1,1}, \ldots, \mathbf{p}_{4,1}, \mathbf{p}_{1,2}, \ldots, \mathbf{p}_{4,2}]$$

to the equations in (10). There exist symmetric eight by eight matrices $\mathbf{A}_{ij}$ such that Eq. (10) reads

$$[\xi_0, \ldots, \xi_3, \eta_0, \ldots, \eta_3] \cdot \mathbf{A}_{ij} \cdot [\xi_0, \ldots, \xi_3, \eta_0, \ldots, \eta_3]^{\mathrm{T}} = 0.$$

The transformed equations are

$$[\xi_0, \ldots, \xi_3, \eta_0, \ldots, \eta_3] \cdot (\mathbf{P}^{-1})^{\mathrm{T}} \mathbf{A}_{ij} \mathbf{P}^{-1} \cdot [\xi_0, \ldots, \xi_3, \eta_0, \ldots, \eta_3]^{\mathrm{T}} = 0. \tag{11}$$

Remark 4. It is possible to compute symbolically the system of algebraic equations of SM_3 without specifying the DH-parameters of the $3R$-robot. On current PCs with standard hard- and software this pre-processing can be done in short time.

4.3. Intersection of hyper-planes

A 3-space in the seven dimensional projective kinematic image space is geometrically determined by intersecting four hyper-planes $H_1, \ldots, H_4$. Algebraically this means it is given by four linear equations. We will describe every 3-space $T(v_3)$ in this way. The Segre manifold is then the intersection of four hyper-planes, each depending on the parameter v_3. This representation will be used in the proposed algorithm for the inverse kinematics of an open $6R$-chain in Section 5.

For each of the four hyper-planes $H_j(v_3)$ four points $\mathbf{p}_i(v_3)$ are given; but they do not determine $H_j(v_3)$. Because seven points span a hyper-plane in P^7 we need three more points $\mathbf{a}_{j,1}$, $\mathbf{a}_{j,2}$, $\mathbf{a}_{j,3} \in H_j(v_3)$ to compute a linear equation of $H_j(v_3)$. In principle, the points $\mathbf{a}_{j,k}$ can be taken anywhere in P^7 but it makes sense to choose them such that the resulting hyper-plane equations become as simple as possible. Without loss of generality we take the three points such that $\mathbf{a}_{j,k} \in SM_3 \cap S_6^2$. We choose the points $\mathbf{a}_{j,k}$ independent of v_3; there exist fixed parameter values v_3^{jk} such that $\mathbf{a}_{j,k} \in T(v_3^{jk})$.

The points $\mathbf{p}_i(v_3)$ and $\mathbf{a}_{j,k}$ have coordinate vectors

$$\mathbf{p}_i(v_3) = [p_{i0}, \ldots, p_{i7}]^{\mathrm{T}}, \quad \mathbf{a}_{j,k} = [a_0^{jk}, \ldots, a_7^{jk}]^{\mathrm{T}}.$$

Note that the coordinates of $\mathbf{p}_i$ depend linearly on v_3, although this does not reflect in our notation. The equation of a hyper-plane $H_j(v_3)$ is given by the Grassmannian determinant

$$H_j(v_3): \quad \det \begin{bmatrix} x_0 & x_1 & x_2 & x_3 & y_0 & y_1 & y_2 & y_3 \\ p_{10} & p_{11} & p_{12} & p_{13} & p_{14} & p_{15} & p_{16} & p_{17} \\ \vdots & & & & & & & \vdots \\ p_{40} & p_{41} & p_{42} & p_{43} & p_{44} & p_{45} & p_{46} & p_{47} \\ a_0^{j1} & a_1^{j1} & a_2^{j1} & a_3^{j1} & a_4^{j1} & a_5^{j1} & a_6^{j1} & a_7^{j1} \\ a_0^{j2} & a_1^{j2} & a_2^{j2} & a_3^{j2} & a_4^{j2} & a_5^{j2} & a_6^{j2} & a_7^{j2} \\ a_0^{j3} & a_1^{j3} & a_2^{j3} & a_3^{j3} & a_4^{j3} & a_5^{j3} & a_6^{j3} & a_7^{j3} \end{bmatrix} = 0. \tag{12}$$

We denote the coefficients of the hyper-plane equation (12) by c_{jl}, i.e.,

$$H_j(v_3): \; c_{j0}x_0 + c_{j1}x_1 + c_{j2}x_2 + c_{j3}x_3 + c_{j4}y_0 + c_{j5}y_1 + c_{j6}y_2 + c_{j7}y_3 = 0. \tag{13}$$

The coefficients c_{jl} are polynomials of degree four in v_3 and can be interpreted as homogeneous coordinates for the hyper-plane H_j. Because of the special choice of the points $\mathbf{a}_{j,k}$, the polynomials c_{jl} have the common divisor

$$g = (v_3 - v_3^{j1})(v_3 - v_3^{j2})(v_3 - v_3^{j3}). \tag{14}$$

Dividing the polynomials c_{jl} by g yields hyper-plane coordinates for $H_j(v_3)$ that depend linearly on v_3. We state this as

Theorem 5. *The Segre manifold* SM_3 *is the intersection of four one parameter pencils of hyper-planes* $H_j(v_3)$. *The hyper-plane coordinates of* $H_j(v_3)$ *depend linearly on* v_3.

Remark 6. It is even possible to compute symbolically the hyper-plane coordinates of $H_j(v_3)$ without specifying the DH-parameters of the $3R$-robot. Computed once the equations can be taken for every possible design.

It is not necessary to compute the common divisor g of Eq. (14) by an appropriate choice of the points $\mathbf{a}_{j,k}$. If we let $u_3 = \pi$, i.e., $v_3 = \infty$, the determinant (12) will be only of degree one in v_3. This can be seen as follows:

We divide Eq. (13) by v_3^4. In the limit $v_3 \to \infty$ all but the leading coefficients of c_{jk} vanish. Hence, $v_3 = \infty$ can be regarded as a common zero of multiplicity three of the coefficients of the hyper-plane coordinates of H_j.

5. Discussion of the inverse kinematics of general 6*R* manipulators

In this section we show how the constraint manifolds of $3R$-chains can be used to solve the inverse kinematics of a general open $6R$ manipulator. Recall that in the inverse kinematic problem of a serial chain the design and a pose of the end-effector of the manipulator is known. The rotation angles u_i of the revolute joints have to be computed. To apply the theory developed in the last sections we break up the link between the third and the fourth revolute joint of the $6R$ and attach two copies of a coordinate frame $\Sigma_\mathrm{L} = \Sigma_\mathrm{R}$ (the "left" and the "right" frame) in the middle of the common normal of these two joints such, that the twist angle between the z-axis of Σ_3 and $\Sigma_\mathrm{L} = \Sigma_\mathrm{R}$ is $\frac{\alpha_3}{2}$ (Fig. 3). Then we compute the direct kinematics for the first half of the $6R$ manipulator, which is now a $3R$-chain, with the end-effector frame Σ_L. The pose of Σ_L with respect to Σ_0 is given by

$$\mathbf{T}_1 = \mathbf{M}_1 \cdot \mathbf{G}_1 \cdot \mathbf{M}_2 \cdot \mathbf{G}_2 \cdot \mathbf{M}_3 \cdot \mathbf{G}_{31}, \quad \mathbf{G}_{31} = \begin{bmatrix} 1 & 0 & 0 & 0 \\ \frac{a_3}{2} & 1 & 0 & 0 \\ 0 & 0 & \cos\left(\frac{\alpha_3}{2}\right) & -\sin\left(\frac{\alpha_3}{2}\right) \\ d_3 & 0 & \sin\left(\frac{\alpha_3}{2}\right) & \cos\left(\frac{\alpha_3}{2}\right) \end{bmatrix}. \tag{15}$$

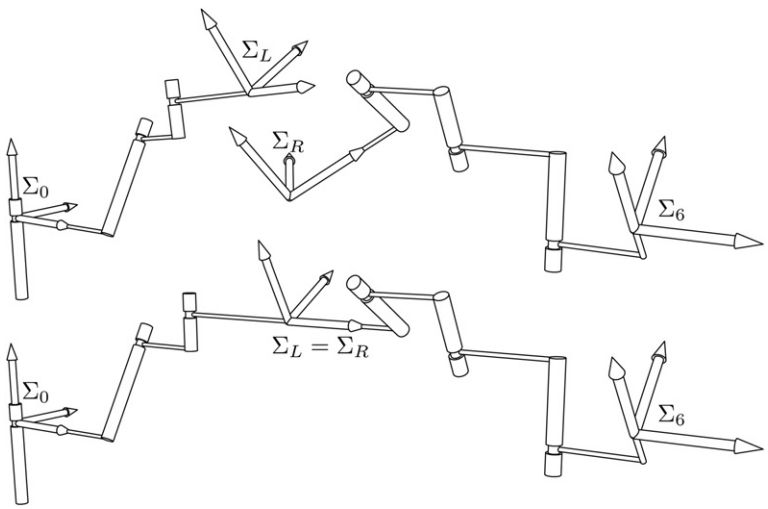

Fig. 3. Cutting of the $6R$ into two $3R$ serial chains.

When the end-effector of the $6R$ manipulator is fixed we can do the same with the second part of the $6R$ but in the opposite direction. This means that for this $3R$ manipulator Σ_6 is the base and Σ_R is the end-effector frame. Therefore, the pose of Σ_R with respect to Σ_6 is given by

$$\mathbf{T}_2 = \mathbf{A} \cdot \mathbf{G}_6^{-1} \cdot \mathbf{M}_6^{-1} \cdot \mathbf{G}_5^{-1} \cdot \mathbf{M}_5^{-1} \cdot \mathbf{G}_4^{-1} \cdot \mathbf{M}_4^{-1} \cdot \mathbf{G}_{32}^{-1}, \quad \mathbf{G}_{32} = \begin{bmatrix} 1 & 0 & 0 & 0 \\ \frac{a_3}{2} & 1 & 0 & 0 \\ 0 & 0 & \cos\left(\frac{\alpha_3}{2}\right) & -\sin\left(\frac{\alpha_3}{2}\right) \\ 0 & 0 & \sin\left(\frac{\alpha_3}{2}\right) & \cos\left(\frac{\alpha_3}{2}\right) \end{bmatrix}, \tag{16}$$

where $\mathbf{A}$ represents the coordinate transformation from Σ_6 to Σ_0. In some discrete poses Σ_L and Σ_R have to coincide. From literature it is well known that there will be up to 16 such real poses when the given $6R$-chain is general. They are found as the intersection

$$S_6^2 \cap \mathrm{SM}_{3,\mathrm{L}} \cap \mathrm{SM}_{3,\mathrm{R}},$$

where

- S_6^2 is the Study quadric.
- $\mathrm{SM}_{3,\mathrm{L}}$ is the kinematic image of the left $3R$-chain and
- $\mathrm{SM}_{3,\mathrm{R}}$ is the kinematic image of the right $3R$-chain.

$\mathrm{SM}_{3,\mathrm{L}}$ is a Segre manifold in P^7. In Section 4.3 we saw that $\mathrm{SM}_{3,\mathrm{L}}$ is the intersection of four one-parameter sets of hyper-planes. The same is true for $\mathrm{SM}_{3,\mathrm{R}}$. Hence, we have to intersect eight one parameter sets of hyper-planes with S_6^2. We summarize these results in

Theorem 7. *Geometrically the inverse kinematics of a general $6R$ serial chain is equivalent to the intersection of eight one parameter sets $H_i(v_3)$, $H_{i+4}(v_6)$ of hyper-planes with S_6^2 ($i = 1, \ldots, 4$).*

An investigation of the algebraic structure of the nine equations reveals the non-linearity of the problem. We have eight hyper-plane equations $H_i(v_3) = 0$, $H_{i+4}(v_6) = 0$, $i = 1, \ldots, 4$ and Eq. (5) of S_6^2. The equations H_i are linear in x_i, y_i and bilinear in $x_i v_3$ and $y_i v_3$ resp. $x_i v_6$ and $y_i v_6$. The solution algorithm of this system is straight forward.

At first we normalize the Study parameters by setting one suitable coordinate equal to one (at least one Study parameter has to be non-zero!). The remaining seven Study parameters are solved linearly from seven arbitrary H_i equations, say $H_1, \ldots, H_7$. As result we obtain all Study parameters depending on the two parameters v_3 and v_6, i.e., $x_i = x_i(v_3, v_6)$, $y_i = y_i(v_3, v_6)$. Substituting x_i and y_i in the one remaining equation H_8 and in Eq. (5) we obtain two non-linear algebraic equations $E_1(v_3, v_6) = 0$, $E_2(v_3, v_6) = 0$.

Remark 8. The vanishing of E_1 is the condition for intersecting three-spaces $T_\mathrm{L}(v_3)$ and $T_\mathrm{R}(v_6)$ of the left and the right Segre manifold. Hence, it can also be written as

$$\det[\mathbf{p}_{1\mathrm{L}}, \mathbf{p}_{2\mathrm{L}}, \mathbf{p}_{3\mathrm{L}}, \mathbf{p}_{4\mathrm{L}}, \mathbf{p}_{1\mathrm{R}}, \mathbf{p}_{2\mathrm{R}}, \mathbf{p}_{3\mathrm{R}}, \mathbf{p}_{4\mathrm{R}}] = 0,$$

where $\mathbf{p}_{i\mathrm{L}} = \mathbf{p}_{i\mathrm{L}}(v_3)$ and $\mathbf{p}_{j\mathrm{R}} = \mathbf{p}_{j\mathrm{R}}(v_6)$ are four points that span $T_\mathrm{L}(v_3)$ and $T_\mathrm{R}(v_6)$, respectively.

The resultant of E_1 and E_2 with respect to one unknown yields a univariate polynomial of degree 48 in the remaining unknown. This polynomial factors into a univariate polynomial $\mathscr{P}_1$ of degree 16, in a polynomial $\mathscr{P}_2$ of degree 8 squared and in a polynomial $(1 - v_i^2)^8$, $i = 3$ or $i = 6$ that comes from the half tangent substitution. $\mathscr{P}_1$ yields the solution of the system and $\mathscr{P}_2$ comes from the determinant of the linear system that has been solved before. $\mathscr{P}_2$ would lead to the trivial solution $[0:0:0:0:0:0:0:0:0]^\mathrm{T}$ and therefore it has to be non-zero.

We solve $\mathscr{P}_1$ for the unknown and obtain 16 solutions over $\mathbb{C}$. The solution of the other unknown we obtain by back substitution in E_1 and E_2. Solving both equations and comparing the solutions yields one common solution of the system. Note that the solutions of the unknowns v_3 and v_6 are already the algebraic values of the joint angles of joint three and six. Having the values of v_3 and v_6 the poses of the middle coordinate system $\Sigma_\mathrm{L} = \Sigma_\mathrm{R}$ can be computed with the corresponding Study parameters.

The remaining task is simple: We have to compute the joint angles of two $2R$-chains, given the pose of the end effector. We know the matrices $\widetilde{\mathbf{T}}_1(u_1, u_2)$, $u_3 = \text{const.}$ and $\widetilde{\mathbf{T}}_2(u_4, u_5)$, $u_6 = \text{const.}$ that describe the motion of these chains. Therefore we have to compare the entries of the two motion matrices with the entries of the matrix that describes the pose of the end effector of the $2R$-chains. This leads to an over-constrained set of equations for the four unknown angles of the chains. It turns out that (in the general case) we get for every pair of angles u_3 and u_6 corresponding to the algebraic values v_3 and v_6 exactly one quadruple of angles u_1, u_2, u_4 and u_5.

The whole algorithm yields 16 sets of angles for the revolute joints of the general $6R$ serial chain and therefore solves the inverse kinematics problem.

Algorithm 1 (*Inverse kinematics of a general* $6R$-chain).

Input: $6R$-chain by its DH-parameters, the pose of an end-effector.
Output: 16 sets of rotation angles that yield the given end-effector pose.

(1) According to Section 5, Eqs. (15) and (16) compute the pose of Σ_{L} (the "left middle frame") of the $6R$-chain, with respect to Σ_0 (the "left" $3R$-chain) and the pose of Σ_{R} (the "right middle frame") with respect to Σ_6 (the "right" $3R$-chain).
(2) Compute four parametric representations $\mathbf{p}_1(v_3), \ldots, \mathbf{p}_4(v_3)$ of straight lines in the kinematic image of the left $3R$-chain (see Section 3). Do the same for the right $3R$-chain, obtaining four parametric representations $\mathbf{q}_1(v_6), \ldots, \mathbf{q}_4(v_6)$.
(3) Use the parametric representations $\mathbf{p}_i(v_3)$ and $\mathbf{q}_j(v_6)$ to compute algebraic equations for the hyper-planes $H_1(v_3), \ldots, H_4(v_3)$ and $H_5(v_6), \ldots, H_8(v_6)$ according to Eq. (12).
(4) Intersect the hyper-planes $H_1(v_3), \ldots, H_4(v_3)$ and $H_5(v_6), \ldots, H_7(v_6)$. This yields a point $\mathbf{r}(v_3, v_6)$, depending on the two parameters v_3 and v_6.
(5) Substitute $\mathbf{r}(v_3, v_6)$ in the equation of $H_8(v_6)$ and Eq. (5) of the Study quadric. This yields two algebraic equations E_1, E_2 in v_3 and v_6.
(6) Compute the resultant R of E_1 and E_2 with respect to v_3. The resultant is a polynomial that can be written as

$$R = (1 + v_6^2)^8 \cdot \mathscr{P}_1(v_6) \cdot \mathscr{P}_2(v_6)^2.$$

In this equation, $\mathscr{P}_2(v_6)$ and $\mathscr{P}_1(v_6)$ are polynomials of respective degree eight and 16. The roots $v_{6,1}, \ldots, v_{6,16}$ of $\mathscr{P}_1(v_6)$ are the possible solutions for v_6 and lead directly to the 16 joint angles via $u_{6,i} = 2\arctan v_{6,i}$.
(7) Insert $v_{6,i}$ into E_1 and E_2 and compute the unique common solution $v_{3,i}$ of the resulting algebraic equations in v_3.
(8) Let $\mathbf{r}_i = \mathbf{r}(v_{3,i}, v_{6,i})$. The points $\mathbf{r}_i$ are the kinematic images of those poses where $\Sigma_{\mathrm{L}} = \Sigma_{\mathrm{R}}$.
(9) Solving the inverse kinematics of the remaining "left" and "right" $2R$-chain yields all missing joint angles.

Remark 9. It is possible that the Segre manifold SM_3 is not suited for the algorithm. If, for example, the first and second revolute axes are parallel or intersecting, the two parameter motion obtained by fixing u_3 of the "left" $3R$-chain is planar or spherical. As a consequence, SM_3 is completely contained in S_6^2. In this case we have to replace SM_3 by one of the Segre manifolds SM_3' or SM_3'', obtained by fixing the first or the second revolute angle.[2]

Remark 10. If all three revolute axes of a $3R$-chain are intersecting (wrist partitioned manipulator) or parallel, the Segre manifold SM_3 degenerates to a single 3-space on the Study quadric S_6^2. In this case our algorithm is even simpler: we just have to intersect four one parameter sets of hyper-planes with a fixed 3-space.

[2] Note that some of the well known industrial manipulators have this feature. We emphasize that nevertheless the algorithm works. We just have to take another Segre manifold.

6. Conclusion

A new algorithm to compute the inverse kinematics of general $6R$-chains was presented. Using multidimensional geometry and classical theory of Segre manifolds for the first time the geometric nature of the problem was revealed. The efficiency of the developed theory is demonstrated in a numerical example in Appendix A. It is believed that this algorithm can be successfully applied to all different $6R$-chains and that it can be completely automatized. This step is subject to further research.

Appendix A. Numerical example

In this appendix we illustrate our algorithm at hand of a numerical example.

A.1. Parameters of the given manipulator

The design of the $6R$ robot is given by the Denavit Hartenberg parameters:

$$\begin{aligned}&\alpha_1 = -\frac{\pi}{6}, \quad \alpha_2 = \frac{\pi}{6}, \quad \alpha_3 = \frac{\pi}{3}, \quad \alpha_4 = -\frac{\pi}{6}, \quad \alpha_5 = -\frac{\pi}{6}, \quad \alpha_6 = \frac{\pi}{4}, a_1 = 10,\\ &a_2 = 100, \quad a_3 = 150, \quad a_4 = 20, \quad a_5 = 5, \quad a_6 = 20,\\ &d_1 = 100, \quad d_2 = 50, \quad d_3 = 50, \quad d_4 = -50, \quad d_5 = -20, \quad d_6 = 10.\end{aligned}$$

To verify the algorithm above we compute one pose of the end effector with a set of "nice" parameters of the revolute joints. We set

$$u_1 = -\frac{\pi}{6}, \quad u_2 = \frac{\pi}{2}, \quad u_3 = -\frac{\pi}{3}, \quad u_4 = \frac{\pi}{2}, \quad u_5 = \frac{\pi}{6}, \quad u_6 = -\frac{\pi}{6} \tag{A.1}$$

and obtain the matrix $\mathbf{A}$ describing the pose of the end effector:

$$\mathbf{A} = \begin{bmatrix} 1 & 0 & 0 & 0 \\ \frac{3395}{128} + \frac{7005\sqrt{3}}{64} & -\frac{59\sqrt{3}}{512} + \frac{177}{256} & -\frac{\sqrt{2}(114\sqrt{3}+433)}{1024} & \frac{\sqrt{2}(66\sqrt{3}-115)}{1024} \\ \frac{4155\sqrt{3}}{128} + \frac{5455}{64} & \frac{57\sqrt{3}}{256} + \frac{39}{512} & \frac{\sqrt{2}(39\sqrt{3}+122)}{1024} & \frac{\sqrt{2}(21\sqrt{3}-650)}{1024} \\ \frac{1845\sqrt{3}}{64} - \frac{695}{32} & \frac{15\sqrt{3}}{128} + \frac{137}{256} & -\frac{\sqrt{2}(55\sqrt{3}-246)}{512} & \frac{\sqrt{2}(59\sqrt{3}+90)}{512} \end{bmatrix}.$$

A.2. Constraint manifold of the first 3R

In the first step of the algorithm the constraint manifold of the first $3R$ is computed. The matrix $\mathbf{T}_1$ (Eq. (15)) describes the relative position of Σ_L with respect to Σ_0 and depends on the first three joint parameters u_1, u_2 and u_3. According to the algorithm above one 3-space of the constraint manifold of this $3R$-chain is spanned by four points, corresponding to the kinematic images of four poses of the end effector of this chain. We assign values for u_1 and u_2, perform half tangent substitution to get rid of the trigonometric functions and obtain four one parameter sets of kinematic image points:

$$\begin{aligned}\mathbf{p}_1(0,0,v_3) = [&-4 - 2\sqrt{3}, -2, -2v_3, -4v_3 - 2v_3\sqrt{3}, -185 - 400v_3 - 200v_3\sqrt{3}, 370 + 185\sqrt{3} - 100v_3, 200\\ &+ 50\sqrt{3} - 70v_3 - 35v_3\sqrt{3}, 350 + 200\sqrt{3} + 35v_3]^{\mathrm{T}},\end{aligned}$$

$$\begin{aligned}\mathbf{p}_2\left(0,\frac{\pi}{3},v_3\right) = [&-4v_3 - 2v_3\sqrt{3} + 4\sqrt{3} + 6, 2v_3 + 2\sqrt{3}, 2v_3\sqrt{3} + 2\sqrt{3} + 2, 4v_3\sqrt{3} + 2\sqrt{3} + 2 + 6v_3, 585v_3\\ &+ 300 + 385\sqrt{3} + 400v_3\sqrt{3}, -30v_3 - 455 - 270\sqrt{3} + 85v_3\sqrt{3}, 105v_3 - 315 - 365\sqrt{3}\\ &+ 120v_3\sqrt{3}, 165v_3\sqrt{3} - 185\sqrt{3} - 435 + 350v_3]^{\mathrm{T}},\end{aligned}$$

$$\mathbf{p}_3\left(\frac{\pi}{2},0,v_3\right) = [-4v_3 - 2v_3\sqrt{3} + 4 + 2\sqrt{3}, -2v_3 + 2, 2 + 2v_3, 4 + 4v_3 + 2\sqrt{3} + 2v_3\sqrt{3}, 435v_3 + 535 + 200\sqrt{3} + 200v_3\sqrt{3}, 30v_3 - 170 - 135\sqrt{3} - 35v_3\sqrt{3}, 170v_3 - 570 - 235\sqrt{3} + 35v_3\sqrt{3}, 365v_3 - 165 - 200\sqrt{3} + 200v_3\sqrt{3}]^{\mathrm{T}},$$

$$\mathbf{p}_4\left(\frac{\pi}{2},\frac{\pi}{2},v_3\right) = [2 - (8 + 4\sqrt{3})v_3, -2\sqrt{3}, 4v_3 + 4 + 2\sqrt{3}, 4\sqrt{3} + 6, 70v_3 + 670 + 235\sqrt{3}, 95 + 130\sqrt{3} - 100v_3\sqrt{3}, (140 + 70\sqrt{3})v_3 - 635 - 300\sqrt{3}, (400\sqrt{3} + 700)v_3 + 165\sqrt{3} + 300]^{\mathrm{T}}.$$

For a constant parameter value v_3 these points span one 3-space $T(v_3)$ in the kinematic image space. To describe this 3-space we intersect four hyper-planes which are on this 3-space. To obtain one of these hyper-planes we add three arbitrary points $\mathbf{a}_{j,1}$, $\mathbf{a}_{j,2}$ and $\mathbf{a}_{j,3}$, outside of the 3-space and compute the Grassmann determinant to get the equation $H_j(v_3)$. The coefficients of $H_j(v_3)$ are polynomials of degree four in v_3. In order to get a simpler equation of $H_j(v_3)$ we choose the points $\mathbf{a}_{j,1}$, $\mathbf{a}_{j,2}$ and $\mathbf{a}_{j,3}$ in the fixed 3-space $T(\infty)$. Points in $T(\infty)$ are found by substituting arbitrary values of u_1 and u_2 and $u_3 = \pi$ in $\mathbf{T}_1$ (because $v_3 \to \infty$ corresponds to $u_3 \to \pi$ in the half tangent substitution). Then the Grassmann determinant immediately yields equations $H_j(v_3)$ that are linear in v_3.

$$\mathbf{a}_{1,1} = \mathbf{p}\left(0,\frac{\pi}{3},\pi\right) = [-4 - 2\sqrt{3}, 2, 2\sqrt{3}, 6 + 4\sqrt{3}, 585 + 400\sqrt{3}, -30 + 85\sqrt{3}, 105 + 120\sqrt{3}, 350 + 165\sqrt{3}]^{\mathrm{T}},$$

$$\mathbf{a}_{1,2} = \mathbf{p}\left(\frac{\pi}{2},0,\pi\right) = [-8 - 4\sqrt{3}, -4, 4, 4\sqrt{3} + 8, 870 + 400\sqrt{3}, 60 - 70\sqrt{3}, 340 + 70\sqrt{3}, 730 + 400\sqrt{3}]^{\mathrm{T}},$$

$$\mathbf{a}_{1,3} = \mathbf{p}\left(\frac{\pi}{2},\frac{\pi}{2},\pi\right) = [-16 - 8\sqrt{3}, 0, 8, 0, 140, -200\sqrt{3}, 280 + 140\sqrt{3}, 1400 + 800\sqrt{3}]^{\mathrm{T}},$$

$$\mathbf{a}_{2,1} = \mathbf{p}\left(-\frac{\pi}{3},\frac{\pi}{6},-\pi\right) = [-2, 2 - 2\sqrt{3}, 2 - 2\sqrt{3}, -2\sqrt{3} - 4, -355 - 210\sqrt{3}, 40 - 110\sqrt{3}, -160 + 40\sqrt{3}, 110 + 75\sqrt{3}]^{\mathrm{T}},$$

$$\mathbf{a}_{2,2} = \mathbf{p}\left(\frac{\pi}{6},-\frac{\pi}{3},\pi\right) = [-2, -2 + 2\sqrt{3}, 2 - 2\sqrt{3}, -2\sqrt{3} - 4, -305 - 260\sqrt{3}, 60 - 90\sqrt{3}, 90 - 110\sqrt{3}, 160 + 25\sqrt{3}]^{\mathrm{T}},$$

$$\mathbf{a}_{2,3} = \mathbf{p}\left(-\frac{\pi}{6},-\frac{\pi}{3},\pi\right) = [-8 - 4\sqrt{3}, -2 + 2\sqrt{3}, -2 - 2\sqrt{3}, -8 - 4\sqrt{3}, -730 - 450\sqrt{3}, -165 - 115\sqrt{3}, 75 - 105\sqrt{3}, 820 + 400\sqrt{3}]^{\mathrm{T}}.$$

$$\mathbf{a}_{3,1} = \mathbf{p}\left(-\frac{\pi}{3},-\pi,\pi\right) = [-12 - 6\sqrt{3}, 6, -2\sqrt{3}, 4\sqrt{3} + 6, 555 + 350\sqrt{3}, 60 - 45\sqrt{3}, 45 + 180\sqrt{3}, 1050 + 615\sqrt{3}]^{\mathrm{T}},$$

$$\mathbf{a}_{3,2} = \mathbf{p}\left(\frac{\pi}{6},\pi,\pi\right) = [-14 - 8\sqrt{3}, 4 + 2\sqrt{3}, 2, -2\sqrt{3} - 4, -215\sqrt{3} - 380, -105 - 110\sqrt{3}, 120 + 85\sqrt{3}, 1285 + 750]^{\mathrm{T}},$$

$$\mathbf{a}_{3,3} = \mathbf{p}\left(-\frac{\pi}{6},-\frac{\pi}{3},\pi\right) = [-8 - 4\sqrt{3}, -2 + 2\sqrt{3}, -2 - 2\sqrt{3}, -8 - 4\sqrt{3}, -730 - 450\sqrt{3}, -165 - 115\sqrt{3}, 75 - 105\sqrt{3}, 820 + 400\sqrt{3}]^{\mathrm{T}},$$

$$\mathbf{a}_{4,1} = \mathbf{p}\left(-\frac{\pi}{3},0,\pi\right) = [-2\sqrt{3} - 4, -2, -2\sqrt{3}, -6 - 4\sqrt{3}, -565 - 400\sqrt{3}, -70 - 135\sqrt{3}, -5 - 70\sqrt{3}, 400 + 235\sqrt{3}]^{\mathrm{T}},$$

$$\mathbf{a}_{4,2} = \mathbf{p}\left(0,-\frac{\pi}{3},\pi\right) = [-2\sqrt{3} - 4, 2, -2\sqrt{3}, -6 - 4\sqrt{3}, -615 - 400\sqrt{3}, -30 - 115\sqrt{3}, -105 - 20\sqrt{3}, 350 + 235\sqrt{3}]^{\mathrm{T}},$$

$$\mathbf{a}_{4,3} = \mathbf{p}\left(-\frac{\pi}{6},0,\pi\right) = [-2, -4 + 2\sqrt{3}, -2, -2\sqrt{3} - 4, -330 - 235\sqrt{3}, -135, 130 - 135\sqrt{3}, 235]^{\mathrm{T}}.$$

$$
\begin{aligned}
H_1(v_3) = {} & x_0(879820000\sqrt{3}v_3 + 7997831335\sqrt{3} + 18615630775 - 2458446230v_3) \\
& + x_1(15557665485\sqrt{3} - 10289261725 + (882841230 - 1504944900\sqrt{3})v_3) \\
& + x_2(\sqrt{3}(8765324530v_3 - 10282046735) - 10864007140v_3 - 15539094485) \\
& + x_3(\sqrt{3}(14265570715 + 17086648130v_3) - 20362019865 + 948245440v_3) \\
& + y_0(-81665352v_3 - 21097838\sqrt{3} - 178631836\sqrt{3}v_3 + 28205302) \\
& + y_1(-21097838 - 192562844\sqrt{3}v_3 + 148938168v_3 - 18119382\sqrt{3}) \\
& + y_2(163785002\sqrt{3} - 248011590 + 41281724v_3) \\
& + y_3(-42195676v_3 + 193478670 + 5042960\sqrt{3}v_3 + 137114098\sqrt{3}) = 0, \\
H_2(v_3) = {} & x_0(\sqrt{3}(-111014692455 - 36908859090v_3) - 163990921360 - 54091774350v_3) \\
& + x_1(11731078460v_3 - 952551340\sqrt{3} - 4349708810\sqrt{3}v_3 - 27897733735) \\
& + x_2(\sqrt{3}(-11716981360v_3 + 84696082225) - 40685203670v_3 + 140549969160) \\
& + x_3(\sqrt{3}(-83471736350v_3 + 25596865180) - 153129765650v_3 + 11397817355) \\
& + y_0(824350144\sqrt{3}v_3 - 245876200\sqrt{3} - 414555694 + 1461521816v_3) \\
& + y_1(148507876\sqrt{3}v_3 - 381217586\sqrt{3} + 727713440v_3 - 245876200) \\
& + y_2(364548532v_3 - 507999094 - 48318352\sqrt{3}) \\
& + y_3(-805014846\sqrt{3} - 397886640\sqrt{3}v_3 - 491752400v_3 - 1600381936) = 0, \\
H_3(v_3) = {} & x_0(4214917835\sqrt{3} + 8425162415\sqrt{3}v_3 - 17698709765 - 3644110880v_3) \\
& + x_1(-3971227815v_3 - 22588758935\sqrt{3} + 3496621050\sqrt{3}v_3 + 26010131165) \\
& + x_2(\sqrt{3}(-19962750315v_3 - 9461671465) + 33061744220v_3 + 18084770365) \\
& + x_3(\sqrt{3}(-20143734350v_3 - 34859357735) + 26740524685v_3 + 48621553935) \\
& + y_0(306339240\sqrt{3}v_3 - 53519738\sqrt{3} + 230723422 - 460427418v_3) \\
& + y_1(373401382\sqrt{3}v_3 + 11013742\sqrt{3} - 625210164v_3 - 53519738) \\
& + y_2(98841098v_3 + 790315782 - 465774702\sqrt{3}) \\
& + y_3(43513018\sqrt{3} + 120868582\sqrt{3}v_3 - 107039476v_3 - 146903778) = 0, \\
H_4(v_3) = {} & x_0(2270v_3 + 1000\sqrt{3}v_3 + 3600\sqrt{3} + 7125) \\
& + x_1(1950 - 270\sqrt{3}v_3 - 40v_3 + 75\sqrt{3}) \\
& + x_2(75\sqrt{3}v_3 - 6940 - 3220\sqrt{3} + 1950v_3) \\
& + x_3(1220 + 3600\sqrt{3}v_3 + 7125v_3 - 1000\sqrt{3}) \\
& + y_0(-36\sqrt{3}v_3 - 72v_3 + 10\sqrt{3} + 20) \\
& + y_1(10 - 36v_3) + y_2(36 + 10v_3) + y_3(36\sqrt{3} + 72 + 10\sqrt{3}v_3 + 20v_3) = 0.
\end{aligned}
$$

The intersection of these four pencils of hyper-planes with the Study quadric is the constraint manifold SM_3 of the first half of the $6R$ serial chain.

A.3. Constraint manifold of the second 3R

To get the constraint manifold for the second half of the 6R-chain we have to perform the same procedure with matrix $\mathbf{T}_2$ instead of $\mathbf{T}_1$. Because of limit of space we do not display all the long equations:

$$\begin{aligned}\mathbf{q}_1(0,0,v_6) = [&73726v_6 + 147452 + 60738\sqrt{3} - 6112\sqrt{3}v_6,\\ &77164v_6 - 125678 + 129880\sqrt{3} + 39346\sqrt{3}v_6,\\ &121094v_6 - 22156 - 41638\sqrt{3} - 93208\sqrt{3}v_6,\\ &-28268v_6 + 29414 + 56536\sqrt{3} - 138666\sqrt{3}v_6,\\ &-6929480v_6 + 28673875 - 13788290\sqrt{3} + 1991175\sqrt{3}v_6,\\ &7595115v_6 - 7617080 - 8194855\sqrt{3} + 6728930\sqrt{3}v_6,\\ &-24921680v_6 - 9480285\sqrt{3}v_6 + 65895 + 4944990\sqrt{3},\\ &15725985v_6 + 3220260 + 6158795\sqrt{3} + 51570\sqrt{3}v_6]^{\mathrm{T}},\end{aligned}$$

$$\mathbf{q}_2 = \left(0, \frac{\pi}{3}, v_6\right) = [\cdots]^{\mathrm{T}}, \quad \mathbf{q}_3 = \left(\frac{\pi}{2}, 0, v_6\right) = [\cdots]^{\mathrm{T}}, \quad \mathbf{q}_4\left(\frac{\pi}{2}, \frac{\pi}{2}, v_6\right) = [\cdots]^{\mathrm{T}}.$$

The other points that span the hyper-planes are

$$\begin{aligned}\mathbf{q}_{1,1} = \mathbf{q}\left(\frac{\pi}{3}, \pi, \pi\right) = \Big[&4328 + 1700\sqrt{3}, -1100 + 808\sqrt{3}, -1712 - 92\sqrt{3},\\ &-1316 - 256\sqrt{3}, 112765 - 137375\sqrt{3}, 7505 - 143365\sqrt{3},\\ &-325905 - 163005\sqrt{3}, 54195\sqrt{3} - 5335\Big]^{\mathrm{T}},\end{aligned}$$

$$\mathbf{q}_{1,2} = \mathbf{q}\left(-\frac{\pi}{3}, \frac{\pi}{3}, \pi\right), \quad \mathbf{q}_{1,3} = \mathbf{q}\left(-\frac{\pi}{3}, \frac{\pi}{3}, \pi\right),$$

$$\mathbf{q}_{2,1} = \mathbf{q}\left(-\frac{\pi}{3}, \frac{\pi}{6}, \pi\right), \quad \mathbf{q}_{2,2} = \mathbf{q}\left(\frac{\pi}{6}, -\frac{\pi}{3}, \pi\right), \quad \mathbf{q}_{2,3} = \mathbf{q}\left(-\frac{\pi}{6}, -\frac{\pi}{3}, \pi\right),$$

$$\mathbf{q}_{3,1} = \mathbf{q}\left(-\frac{\pi}{3}, -\frac{\pi}{6}, \pi\right), \quad \mathbf{q}_{3,2} = \mathbf{q}\left(\frac{\pi}{6}, \pi, \pi\right), \quad \mathbf{q}_{3,3} = \mathbf{q}\left(-\frac{\pi}{6}, -\frac{\pi}{3}, \pi\right),$$

$$\mathbf{q}_{4,1} = \mathbf{q}\left(-\frac{\pi}{3}, 0, \pi\right), \quad \mathbf{q}_{4,2} = \mathbf{q}\left(0, -\frac{\pi}{3}, \pi\right), \quad \mathbf{q}_{4,3} = \mathbf{q}\left(-\frac{\pi}{6}, 0, \pi\right),$$

$$\begin{aligned}H_5(v_6) = &-1366845x_1\sqrt{3} - 16788y_1 + 1592995x_2\sqrt{3} - 14046y_2 + 48y_0\sqrt{3}\\ &- 9992y_2\sqrt{3} - 698135x_1 + 2328655x_2 + 14046y_3\sqrt{3} + 28092y_0v_6 - 3091215x_2v_6\\ &- 1110595x_0\sqrt{3} - 169985x_0v_6\sqrt{3} - 458955x_1v_6\sqrt{3} - 1761015x_2v_6\sqrt{3} + 455305x_0\\ &+ 12230y_0 + 20044y_3 - 986y_1\sqrt{3} - 1036125x_1v_6 + 1632925x_3 + 630255x_3\sqrt{3}\\ &- 774385x_0v_6 - 8466y_3v_6 + 4636y_2v_6 + 4966y_1v_6 + 15018y_0\sqrt{3}v_6 + 340695x_3v_6\\ &- 381055x_3\sqrt{3}v_6 - 8370y_2\sqrt{3}v_6 - 6608y_3\sqrt{3}v_6 = 0,\end{aligned}$$

$$H_6(v_6) = \cdots = 0, \quad H_7(v_6) = \cdots = 0, \quad H_8(v_6) = \cdots = 0.$$

A.4. Pose of $\Sigma_L = \Sigma_R$

Now, eight one parametric pencils of hyper-planes ($H_1(v_3), H_2(v_3), H_3(v_3), H_4(v_3)$ and $H_5(v_6), H_6(v_6), H_7(v_6), H_8(v_6)$) are given and we have to intersect these eight pencils with S_6^2 to get the poses where Σ_{L} and Σ_{R} coincide. Intersecting seven of the hyper-planes means solving seven linear equations in x_i, y_i, $i = 0, \ldots, 3$. Remember, x_i, y_i are homogeneous, so one of the Study parameters can be normalized to one. Substituting the solutions in the remaining eighth hyper-plane and in S_6^2 yields two non-linear equations $E_1(v_3, v_6)$ and $E_2(v_3, v_6)$ which are of bi-degree four resp. six.

Equation E_1 has a geometric meaning. It gives us the parameter values, for which the two Segre manifolds (or the eight hyper-planes) intersect. So it can also be generated by the determinant of the matrix:

$$\begin{aligned}
E_1 &= \det[\mathbf{p}_1(u_3), \ldots, \mathbf{p}_4(u_3), \mathbf{q}_1(u_6), \ldots, \mathbf{q}_4(u_6)] = 127961043861390176\sqrt{3} \\
&\quad + 695430062705310720\sqrt{3}v_3 - 869347902378014720v_3v_6^3 - [\ldots 45 \text{ terms} \ldots] = 0, \\
E_2 &= -465742063219970713719653422405377996 00v_3^3 \\
&\quad - 811672683480228781253171750461169420 12v_3^4\sqrt{3}v_6^3 - [\ldots 95 \text{ terms} \ldots] = 0.
\end{aligned}$$

The resultant of these two equations, by eliminating v_3, yields a univariate polynomial in v_6 of degree 48 which can be factored into a polynomial $\mathscr{P}_1$ of degree 16, a polynomial $\mathscr{P}_2^2$ of degree eight squared and in $(1+v_6^2)^8$. Because of the "nice" values for the example $\mathscr{P}_1$ factors in a polynomial of degree one, yielding the solution for the joint parameter of the sixth joint of the set of joint angles we started with and a polynomial of degree 15. The 16 roots of $\mathscr{P}_1$ are

$$\begin{aligned}
v_6 \in \{&-0.2679491920, -0.1651548583, -0.1310929573 \pm 0.8370455908\mathrm{i}, -0.05048057402 \\
&\pm 1.050657450\mathrm{i}, 0.02205333535 \pm 1.054814962\mathrm{i}, 0.02709648159 \pm 0.9336471816\mathrm{i}, 0.1015095637 \\
&\pm 1.085505997\mathrm{i}, 0.1313072143 \pm 0.2075318817\mathrm{i}, 0.2310214712 \pm 0.2195257104\mathrm{i}\}.
\end{aligned}$$

Back substituting one value for v_6 in the equations E_1 and E_2, solving for v_3 and taking the common solution every value of v_6 yields exactly one value for v_3. The 16 solutions for v_3 are

$$\begin{aligned}
v_3 \in \{&-0.5773502693, -0.5513075395, -0.7426315981 \pm 0.8394355258\mathrm{i}, -0.4728081593 \\
&\pm 0.08258900521\mathrm{i}, 0.2116842781 \pm 0.8023896617\mathrm{i}, 0.3899070234 \pm 4.124398357\mathrm{i}, 0.3980795285 \\
&\pm 0.2213303775\mathrm{i}, 0.5648941737 \pm 2.233721302\mathrm{i}, 0.6413657826 \pm 0.1234273129\mathrm{i}\}.
\end{aligned}$$

We can see here, that the first values $(-0.2679491920, -0.5773502693)$ in the two lists are exactly the values for $-\tan\frac{\pi}{12}$ and $-\tan\frac{\pi}{6}$, corresponding to the given angles $u_6 = -\frac{\pi}{6}$ and $u_3 = -\frac{\pi}{3}$ (compare Eq. (A.1)).

We show the back substitution for this set of solutions. Substituting these two angles in the $3R$-chains we have two $2R$-chains for which we know the coinciding poses of the end-effectors. We also know the matrices that describe the motions of these two chains. These are exactly the same matrices as for the two $3R$-chains with the exception that the angles u_3 and u_6 are now fixed. We substitute the value of u_3 in $\mathbf{T}_1$ and the corresponding value of u_6 in $\mathbf{T}_2$ to describe the motion of the $2R$-chains.

$$\widetilde{\mathbf{T}}_1(u_1,u_2) = \begin{bmatrix} t_{11}^1(u_1,u_2) & \cdots & t_{14}^1(u_1,u_2) \\ \vdots & & \vdots \\ t_{41}^1(u_1,u_2) & \cdots & t_{44}^1(u_1,u_2) \end{bmatrix},$$

$$\widetilde{\mathbf{T}}_2(u_4,u_5) = \begin{bmatrix} t_{11}^2(u_4,u_5) & \cdots & t_{14}^2(u_4,u_5) \\ \vdots & & \vdots \\ t_{41}^2(u_4,u_5) & \cdots & t_{44}^2(u_4,u_5) \end{bmatrix}.$$

The pose of the end-effector of the two $2R$-chains ($\Sigma = \Sigma_{\mathrm{L}} = \Sigma_{\mathrm{R}}$) is obtained by back substituting the solutions of v_3 and v_6 in the solutions of the linear system of equations to determine the Study parameters of this pose. We obtain the matrix:

$$\mathbf{T} = (t_{ij}) = \begin{bmatrix} 1 & 0 & 0 & 0 \\ 153.7703938 & 0.7577722258 & 0.3788861134 & 0.5312499911 \\ 83.83813443 & -0.1874999986 & 0.9062500197 & -0.3788861144 \\ 83.92626995 & -0.6249999998 & 0.1875000013 & 0.7577722258 \end{bmatrix}.$$

Table A.1
Sixteen solutions of the inverse kinematics

	u_1	u_2	u_3	u_4	u_5	u_6
Solution 1	−0.524	1.570	−1.047	1.570	0.524	−0.524
Solution 2	−0.624	1.640	−1.008	1.707	0.272	−0.327
Solution 3	−0.873 + 1.357i	0.477 − 1.715i	1.150 + 0.175i	0.710 − 1.220i	0.555 + 1.963i	−0.749 − 2.175i
Solution 4	−0.873 − 1.357i	0.477 + 1.715i	1.150 − 0.175i	0.710 + 1.220i	0.555 − 1.963i	−0.749 + 2.175i
Solution 5	1.360 − 0.766i	1.010 + 1.942i	−1.742 − 0.960i	0.093 + 3.057i	2.977 + 0.004i	−2.383 − 3.356i
Solution 6	1.360 + 0.766i	1.010 − 1.942i	−1.742 + 0.960i	0.093 − 3.057i	2.977 − 0.004i	−2.383 + 3.356i
Solution 7	−0.813 + 1.377i	3.041 − 3.846i	3.093 + 0.490i	1.969 + 4.311i	2.872 − 0.095i	2.770 − 3.549i
Solution 8	−0.813 − 1.377i	3.041 + 3.846i	3.093 − 0.490i	1.969 − 4.311i	2.872 + 0.095i	2.770 + 3.549i
Solution 9	2.417 − 1.477i	2.394 + 4.353i	2.885 − 0.883i	−2.709 − 4.845i	0.204 + 2.443i	0.402 − 3.295i
Solution 10	2.417 + 1.477i	2.394 − 4.353i	2.885 + 0.883i	−2.709 + 4.845i	0.204 − 2.443i	0.402 + 3.295i
Solution 11	−1.390 + 1.849i	2.467 − 2.308i	0.937 + 1.835i	2.699 − 2.228i	−0.268 + 2.647i	2.319 − 2.756i
Solution 12	−1.390 − 1.849i	2.467 + 2.308i	0.937 − 1.835i	2.699 + 2.228i	−0.268 − 2.647i	2.319 + 2.756i
Solution 13	−1.289 − 0.467i	2.211 + 0.523i	−0.888 − 0.135i	1.929 − 0.612i	−0.145 + 1.032i	0.273 − 0.414i
Solution 14	−1.289 + 0.467i	2.211 − 0.523i	−0.888 + 0.135i	1.929 + 0.612i	−0.145 − 1.032i	0.273 + 0.414i
Solution 15	−0.885 − 1.418i	0.873 + 1.359i	0.788 + 0.384i	1.993 − 1.438i	−0.563 + 2.088i	0.475 − 0.422i
Solution 16	−0.885 + 1.418i	0.873 − 1.359i	0.788 − 0.384i	1.993 + 1.438i	−0.563 − 2.088i	0.475 + 0.422i

Now we compare entries of the matrices $\widetilde{\mathbf{T}}_1$ and $\widetilde{\mathbf{T}}_2$ with the entries of the matrix $\mathbf{T}$. This gives 12 equations for the angles u_1 and u_2, resp. u_4 and u_5 and the common solutions of all equations yield, for every pair of values of v_3 and v_6, exactly one value for each angle u_1, u_2, u_4 and u_5. The equations

$$t^1_{24} = t_{24}, \quad t^1_{23} = t_{23}, \quad t^1_{22} = t_{22}, \quad t^1_{31} = t_{31}$$

have the solution $u_1 = -0.5235988065\left(\approx -\frac{\pi}{6}\right)$, $u_2 = 1.570796143\left(\approx \frac{\pi}{2}\right)$ in common. The equations

$$t^2_{44} = t_{4,4}, \quad t^2_{43} = t_{4,3}, \quad t^2_{34} = t_{3,4}, \quad t^2_{33} = t_{3,3}$$

have the solution $u_4 = 1.570796143\left(\approx \frac{\pi}{2}\right)$, $u_5 = 0.5235988065\left(\approx \frac{\pi}{6}\right)$ in common. The complete set of all 16 solutions is listed in Table A.1. The angles are given in radians and only three digits are displayed.

References

[1] H. Lee, C. Liang, Displacement analysis of the general 7-link 7RR mechanism, Mechanism and Machine Theory 23 (3) (1988) 219–226.
[2] M. Raghavan, B. Roth, Inverse kinematics of the general 6R manipulator and related linkages, Transactions of the ASME, Journal of Mechanical Design 115 (1990) 228–235.
[3] M. Ghazvini, Reducing the inverse kinematics of manipulators to the solution of a generalized eigenproblem, in: J. Angeles, G. Hommel, Kovács (Eds.), Computational Kinematics, Solid Mechanics and its Applications, vol. 28, Kluwer Academic Publishers, 1993, pp. 15–26.
[4] J. Angeles, Fundamentals of Robotic Mechanical Systems. Theory, Methods and Algorithms, Springer, New York, 1997.
[5] M. Husty, A. Karger, H. Sachs, W. Steinhilper, Kinematik und Robotik, Springer-Verlag, Berlin, Heidelberg, New York, 1997.
[6] J. McCarthy, Geometric Design of Linkages, Interdisciplinary Applied Mathematics, vol. 320, Springer-Verlag, New York, 2000.
[7] J.M. Selig, Geometric Fundamentals of Robotics, Monographs in Computer Science, Springer, New York, 2005.
[8] E. Study, Geometrie der Dynamen, B.G. Teubner, Leipzig, 1903.
[9] K. Brunnthaler, H.-P. Schröcker, M.L. Husty, A new method for the synthesis of Bennet mechanisms, in: Proceedings of CK 2005, Cassino, Italy, 2005.
[10] J. Naas, H. Schmid, Mathematisches Wörterbuch, vol. Band II, Akademie-Verlag, Berlin, 1974.
[11] J. Harris, Algebraic Geometry: A First Course, Graduate Texts in Mathematics, vol. 133, Springer, 1995.